Saturation of the Nuclear Magnetic Resonance Absorption and the Spin-Lattice Relaxation Time in Solid Hydrogen

Saturation of the Nuclear Magnetic Resonance Absorption and the Spin-Lattice Relaxation Time in Solid Hydrogen*

Tadashi SUGAWARA

The Research Institute for Iron, Steel and Other Metals

(Received February 7, 1956)

Synopsis

A new type of anomaly was found in the saturation behavior of the nuclear magnetic resonance absorption in solid hydrogen with various *ortho-para* ratios. In the central peak, the saturation curve showed anomalous dependence on *rf* field and the line width decreased with increasing *rf* field, while in the side peak, they were of rather normal behaviors. The spin-spin and spin-lattice interactions were discussed in detail and a possible explanation of the anomalies was obtained. They could be interpreted as a sort of inhomogenous saturation. The relaxation times in the side peak and in the central peak were calculated from the experimental saturation curves using a saturation formula obtained from the above treatments. It was found that the central peak has relaxation times distributed over a range from milliseconds to seconds with the maximum value inversely proportional to *ortho* concentration and temperature, and that the side peak has, on the contrary, a single relaxation time.

I. Introduction

During the past few years, experimental studis on solid hydrogen have been made by nuclear magnetic resonance[1],[2],[3], specific heat[4],[5] and infrared absorption measurements[6],[7]. From the nuclear magnetic resonance studies, Reif[2] and the present author[3] concluded that the rotational magnetic moment of *ortho* molecules was quenched by an asymmetric crystalline potential due to the neighbor ing molecules, and that the crystalline potential was not the same at the positions of different *ortho* molecules, as the result of the fact that *ortho* and *para* molecules are mixed randomly in the crystal. Hill[4],[5] measured the specific heat down to very low temperatures and found a λ-type anomaly in hydrogen with high *ortho* concentration besides the anomaly due to the lifting of the rotational degeneracy of the *ortho* molecules. His λ-point was in fair agreement with the line-width transition temperature of the nuclear magnetic resonance[3]. Hare et al[6],[7] studied the infrared adsorption in solid hydrogen with various *ortho* concentrations

The 828th report of the Research Institute for Iron, Steel and Other Metals.

A brief account of this work has been reported previously. T. Sugawara, Phys. Rev., **100** (1955), 759.

(1) J. Hatton and B. V. Rollin, Proc. Roy. Soc. (London), **A199** (1949), 222.
(2) F. Reif and E. M. Purcell, Phys. Rev., **91** (1953), 631.
(3) T. Sugawara, Y. Masuda, T. Kanda and E. Kanda, Sci. Rep. RITU **A7** (1955), 67.
T. Sugawara, Y. Masuda, T. Kanda and E. Kanda, Phys. Rev., **95** (1954), 1344 (L).
The line width of the central peak reported in these papers were found to be somewhat smaller than the true width. See footnote of p. 98.
(4) R. W. Hill and B. W. A. Ricketson, Phil. Mag., **45** (1954), 277.
(5) R. W. Hill, Proceedings of the International Conference on Low Temperature Physics (Paris, 1955). 317.
(6) E. J. Allin, W. F. J. Hare and R. E. MacDonald, Phys. Rev., **98** (1955), 554.
(7) W. F. J. Hare, E. J. Allin and H. L. Welsh, Phys. Rev., **99** (1955), 1887.

and showed that the effect of the intermolecular quadrupole interaction was marked, and that the effect varied with the *ortho* concentration.

Several theoretical works concerning the above-mentioned results were reported recently. Tomita[8] considered the λ-transition as a cooperative ordering of *ortho* molecules and estimated the critical temperature using Bragg-Williams and Bethe's approximations. Nakamura[9] pointed out that the quadrupole interaction between *ortho* molecules was responsible for the high temperature anomaly of the specific heat and also for the cooperative ordering of the molecules at low temperatures. His theoretical value of the specific heat is in good agreement with the experimental value of Hill.

In these theoretical works solid hydrogen was considered as a homogenous solid solution of *ortho* and *para* molecules. As described above, however, the solid should be regarded as an inhomogenous mixture. As a consequence of this fact it may be supposed that the nuclear spin-lattice relaxation time will not be unique in the disordered state in which different *ortho* molecules are rotating in different crystalline potentials. The spin-lattice relaxation time was measured by Hatton and Rollin[1] from the saturation experiments They reported one relaxation time at each temperature in contradiction to the above supposition. Their results were based on a simple saturation theory, which seems to be inadequate in the case of solid hydrogen as will be explained later. The repetition of the saturation experiment would be necessary for the purpose of confirming the validity of our supposition and also to get some informations about the mechanism of spin-lattice relaxation.

II. Previous theory of saturation in solids

The saturation behavior of the nuclear magnetic resonance line was studied extensively by Bloembergen, Purcell and Pound[10]. Their theory is applied well to the saturation in gases, liquid and solids with nuclear motions such as molecular rotation or translational diffusion. Basic assumptions of the BPP theory are, according to Redfield[11], as follows: (1) The dipolar interaction between spins is strong enough so that the absorbed energy can be transfered to all the spins in a short time; (2) Equilibrium of the spin system with the lattice can be attained by the spin-lattice interaction with a characteristic time T_1; (3) The *rf* susceptibility is proportional to the difference in the population of the spin states. According to this simple theory, the imaginary susceptibility χ'' of a system of spin 1/2 is

$$\chi''(\nu, H_1) = \frac{\pi}{2}\chi_0\nu\frac{g(\nu)}{1+\frac{1}{2}\gamma^2H_1^2T_1g(\nu)}, \qquad (1)$$

where χ_0 is the static susceptibility of the nuclear spin system, γ is the magneto-

(8) K. Tomita, Proc. Phys. Soc. (London), **A68** (1955), 213.
(9) T. Nakamura, Prog. Theor. Phys., **14** (1955), 135.
(10) N. Bloembergen, E. M. Purcell and Pound, Phys. Rev., **73** (1948) 679. (henceforth refered to as BPP)
(11) A. G. Redfield, Phys. Rev., **98** (1955), 1787.

mechanical ratio, H_1 is the intensity of the *rf* magnetic field and $g(\nu)$ is the line shape function of the absorption line. Eq. (1) shows that the absorption signal decreases monotonically with increasing H_1 as is observed in many cases.

Recently, Redfield[11] has found that the saturation behavior of the nuclear magnetic resonance line in some solids conflicts with the simple theories of BPP and of F. Bloch[12]. He examined the validity of the three assumptions of the BPP theory and concluded that at high *rf* levels the spin system could not be described by a unique spin temperature in contradiction to the assumption (3). The theory developed by him is in agreement with the observed saturation behavior of the dispersion and absorption signal in powdered aluminum and copper.

Another example which cannot be accounted for by the simple theory is the inhomogeneous saturation observed by Portis[13] in the microwave resonance of F-centers in alkali halides. The absorption signal saturates much easier than the dispersion signal and the saturation curve does not follow the prediction of the simple theory. In this case the overall width of the absorption line is determined by hyperfine interaction of the F-centers with surrounding nuclei. The absorbed energy can be transfered only to the spins whose local fields satisfy the resonance condition. The equilibrium between spins in different local fields can be attained only through spin-lattice interaction. Observed saturation data were in agreement with the theory of inhomogenous saturation given by him.

III. Experimental procedure

Saturation measurements were carried out at 8.2 Mc/sec. by using a *rf* spectrometer of Pound-Watkins type. The block diagram of the experimental arrangement is shown in Fig. 1. The *rf* level at the sample coil was determined from the detector current of a communications receiver coupled to the oscillator through a voltage divider. Calibration of the detector current was made against known *rf* voltage from a signal generator with a reactance attenuator. Derivatives of the absorption signal were obtained on the recorder by sweeping the magnetic field slowly over a necessary range and their heights at various *rf* levels were compared with the calibration signal. The field was modulated at 50-cps with an amplitude of about 0.4 gauss. For the determination of spin-lattice relaxation times, it is necessary to know the relation between the effective value of the *rf* magnetic field

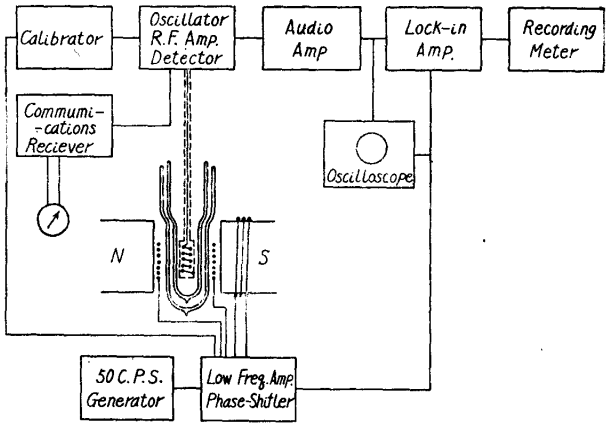

Fig. 1. Block diagram of the experimental arrangement.

(12) F. Bloch, Phys. Rev., **70** (1946), 1.
(13) A. M. Portis Phys. Rev., **91** (1953), 1071.

H_1 and the *rf* voltage at the sample coil. The effective value of H_1 was calculated from Eq. (1) by using the directly observed T_1 of protons at 4.2°K in potassium-aluminum alum containing a known amount of potassium-chromium alum*.

The helium cryostat and the magnet were the same as those used in the previous paper[3].

Hydrogen of low *ortho* concentration was prepared from normal hydrogn by making it contact with activated charcoal at low temperatures. Analysis of the *ortho* concentration of the sample was made before and after the resonance experiment, because the change due to *ortho-para* conversion was considerable during an experimental run.

IV. Experimental results

As stated in the previous paper[3], the absorption line had a single peak ("central peak") at high temperatures. Below a temperature peculiar to the *ortho* concentration of the sample, it became flanked by two side peaks of about 40 gauss separation. When the temperature was further reduced, the intensity of the side peaks increased while that of the central peak decreased. The line shape of the central peak began to change when saturation became appreciable. As an example, the derivative curves at several *rf* levels in 71 per cent *ortho* hydrogen are shown in Fig. 2. The shape of the side peak, on the contrary, remained unchanged up to a considerably high *rf* level.

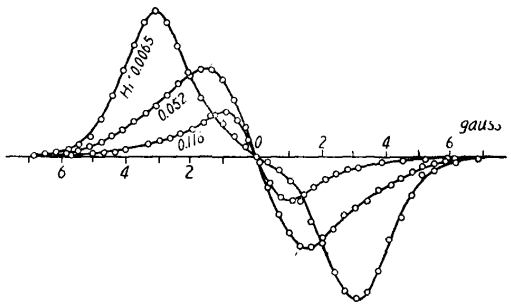

Fig. 2. Derivatives of the adsorption line (central peak) in 71% ortho hydrogen at various values of the *rf* magnetic field intensity.

The line width and the maximum deflection of the derivative of the central peak showed an anomalous behavior as the *rf* level increased from a value which did not produce appreciable saturation. Typical data obtained at 4.2° and 1.25°K are given in Fig. 3 and Fig. 4, respectively. The line width** decreased as the saturation became appreciable and tended to the value characteristic to the *ortho* concentration of the sample. This asymptotic value is, when compared at the same temperature, larger for samples with higher *ortho* concentration. The maximum deflection also showed a complicated behavior against H_1, especially in low concentration hydrogen.

The line width and the maximum deflection of the side peak in 69 per cent hydrogen showed rather normal behavior as seen from Fig. 5. The line width remained unchanged up to the high *rf* level of $H_1 = 0.05$ gauss and then decreased

* T_1 of the alum can be controlled by the amount of Cr^{3+} ion added; see ref. (18).

** It must be noticed that the line width described in the previous paper (ref. (3)) corresponds to the width at partial saturation as the *rf* level of the autodyne used in that experiment was not sufficiently weak enough to give the unsaturtion value.

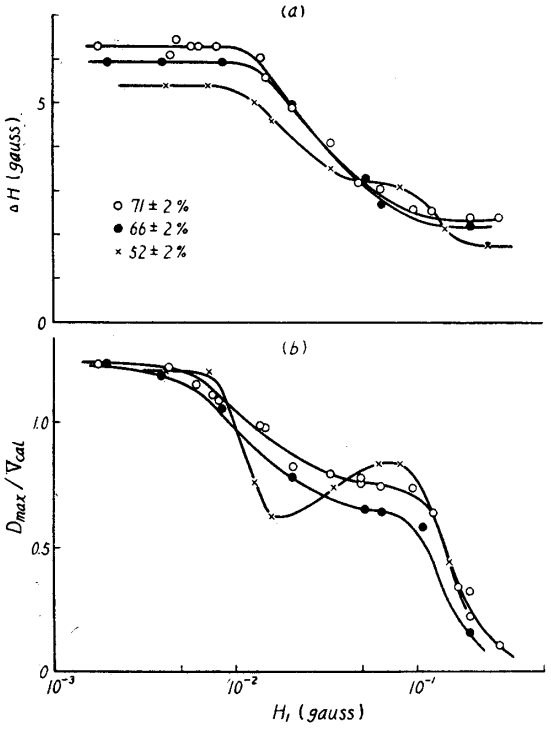

Fig. 3. a) Line width ΔH and b) maximum value $D_{\max}$ of the derivative of the central peak in 71, 66 and 52% ortho hydrogen at 4.2°K as functions of the *rf* magnetic field intensity H_1. The unit of V_{cal} is 1 volt in this and all other figures.

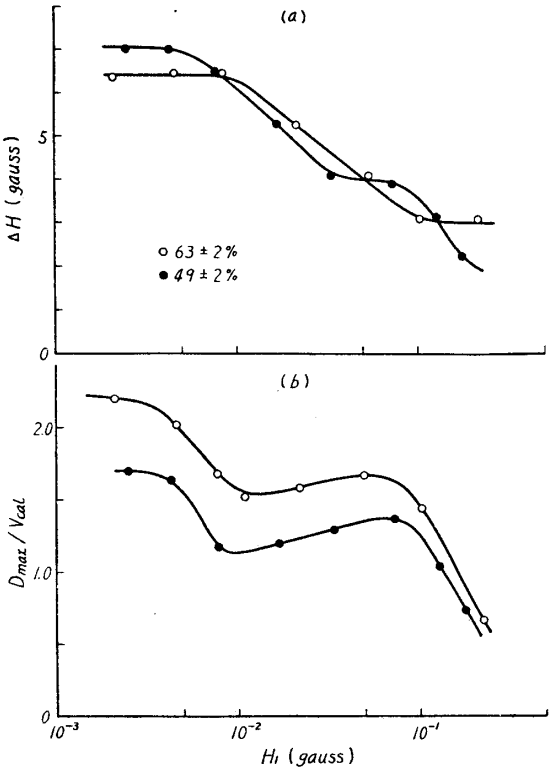

Fig. 4. a) Line width ΔH and b) maximum value $D_{\max}$ of the derivative of the central peak in 63 and 49% ortho hydrogen at 1.25°K as functions of the *rf* magnetic field intensity H_1.

slowly as the level was increased further. The saturation curve (Fig. 5b) resembles to the one expected from Eq. (1) with an assumption of Gaussian line shape[14]. The effect of temperature upon the saturation curve was not found in the range between 1.2°K and the line width transition temperature, i. e. 1.45°K, in 69 per cent hydrogen. The saturation behavior of the central peak coexisting with the side peaks was quite similar to that of the central peak described above. The unsaturated line width of this was about 8 gauss in 69 per cent sample at 1.25°K.

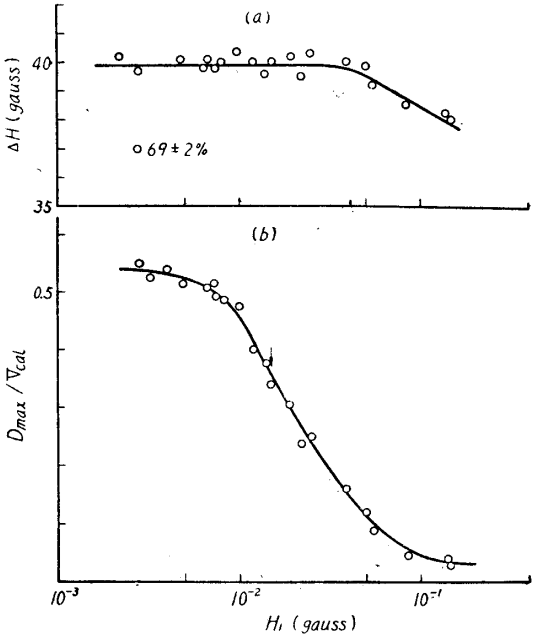

Fig. 5. a) Line width ΔH and b) maximum value $D_{\max}$ of the derivative of the side peak in 69% ortho hydragen at 1.25°K as functions of the *rf* magnetic field intensity H_1.

As the line width of the central

(14) T. Kanda, Jour. Phys. Soc. Jap., **10** (1955), 85.

peak varies with H_1, the saturation curves of Fig. 3b and 4b seem to have no quantitative significance for the purpose of calculating the relaxation time from them. More useful informations will be obtained when the deflections at several distances from the line center on the derivative curve are plotted against H_1. Some of the saturation curves thus obtained are illustrated in Figs. 6~12, in which

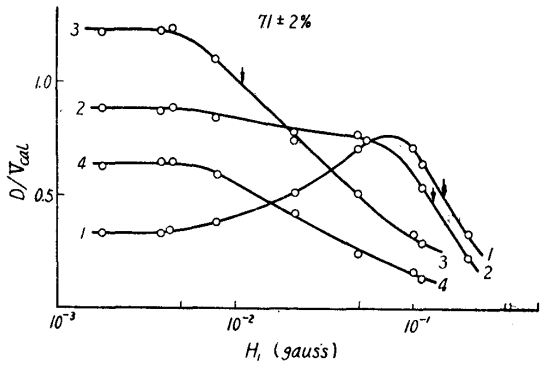

Fig. 6. Saturation curves of components of the central peak in 71% *ort o* hydrogen at 4.2°K. Derivatives at positions separated by 1, 2, 3 and 4 gauss from the line center are shown in curves 1, 2, 3 and 4 as functions of H_1.

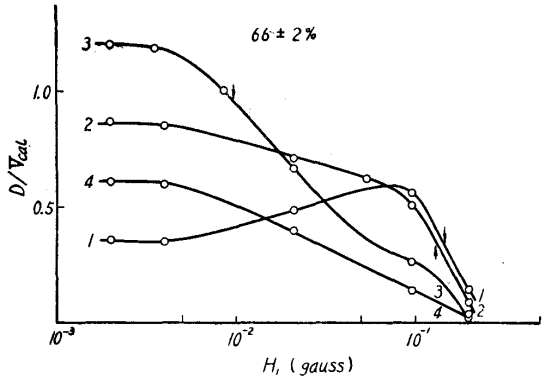

Fig. 7. Saturation curves of the components of the central peak in 66% *ortho* hydrogen at 4.2°K.

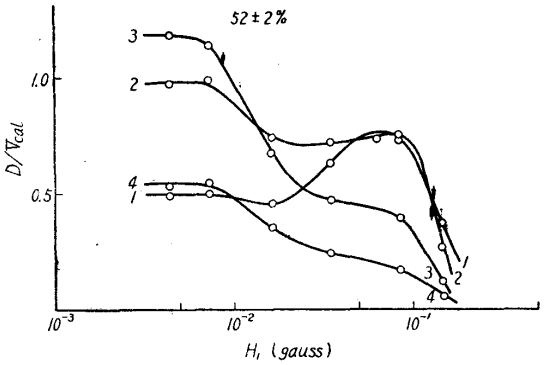

Fig. 8. Saturation curves of the components of the central peak in 52% *ortho* hydrogen at 4.2°K.

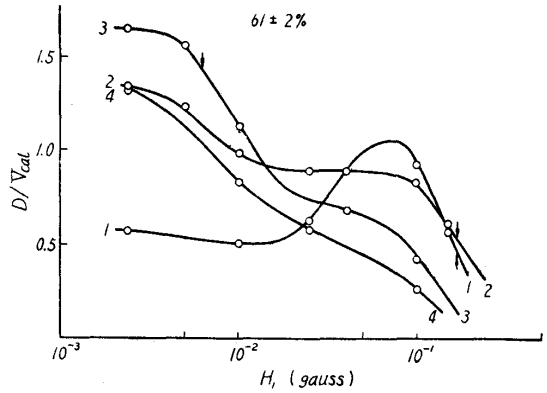

Fig. 9. Saturation curves of the components of the central peak in 61% *ortho* hydrogen at 2.35°K.

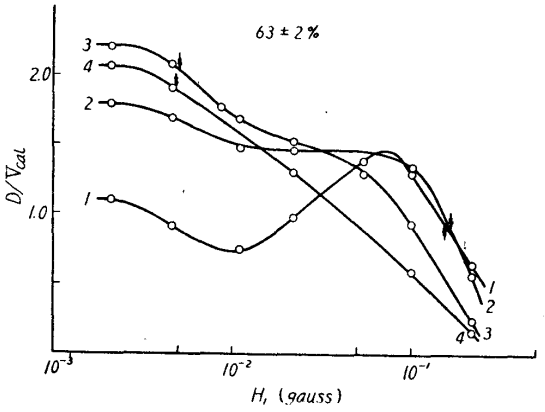

Fig. 10. Saturation curves of the components of the central peak in 63% *ortho* hydrogen at 1.25°K.

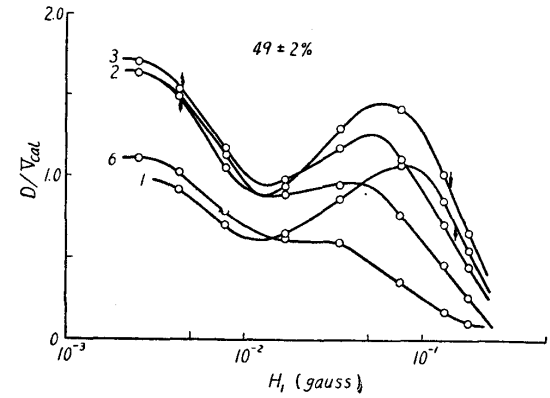

Fig. 11. Saturation curves of the components of the central peak in 49% *ortho* hydrogen at 1.25°K.

the number specifying the individual curve is the distance from the line center expressed in gauss of the corresponding component; for instance, curve 1 is the saturation curve of the component with the distance of 1 gauss from the center. It will be clear from these figures that curves for wide components such as 3 and 4 and those for narrow ones such as 1 show quite different behavior against H_1.

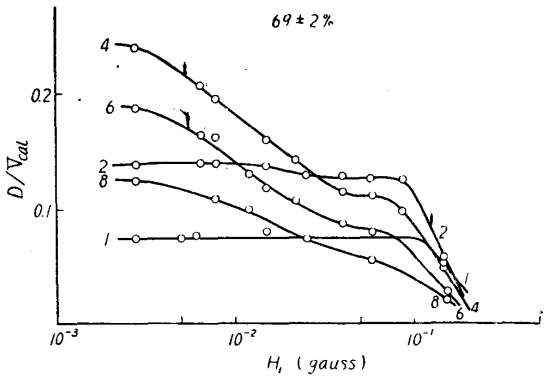

Fig. 12. Saturation curves of the components of the central peak coexisting with the side peak in 69% *ortho* hydrogen at 1.25°K.

If the principal relaxation mechanism is the interaction of nuclei with paramagnetic impurities as is often the case in some insulating crystals, the saturation data will be affected by the content. The possible impurity was oxygen in the present case, which amounted to about 0.05 per cent in tank hydrogen. For samples taken from a tank and those purified by distillation or deoxydization, the saturation curves coincided with one another within the experimental error. Therefore, a small quantity of oxygen seems not to affect the spin-lattice relaxation.

The experimental results are so complicated, as stated above, that a special theory of saturation in solid hydrogen would be required to interpret them. In the following sections, spin-spin and spin-lattice interactions will be discussed from the point of view that the crystal is inhomogeneous, and then the saturation data will be analyzed on the basis of these treatments.

V. Spin-spin interaction

The Hamiltonian of the system in a strong magnetic field is

$$\mathcal{H} = \mathcal{H}_Z + \mathcal{H}_{\rm dip} + \mathcal{H}'_{\rm dip}, \tag{2}$$

with

$$\mathcal{H}_Z = \sum_i \gamma\hbar \mathbf{H}_0 \cdot \mathbf{I}_i, \tag{3}$$

$$\mathcal{H}_{\rm dip} = \sum_i (\gamma\hbar)^2 r_{12}^{-3}[\mathbf{I}_{i1}\cdot\mathbf{I}_{i2} - 3(\mathbf{I}_{i1}\cdot\mathbf{r}_{12})(\mathbf{I}_{i2}\cdot\mathbf{r}_{12})r_{12}^{-2}], \tag{4}$$

$$\mathcal{H}'_{\rm dip} = \sum_{i>j} (\gamma\hbar)^2 r_{ij}^{-3}[\mathbf{I}_i\cdot\mathbf{I}_j - 3(\mathbf{I}_i\cdot\mathbf{r}_{ij})(\mathbf{I}_j\cdot\mathbf{r}_{ij})r_{ij}^{-2}], \tag{5}$$

where $\mathcal{H}_{\rm dip}$ represents the dipolar interaction between two protons in the ith molecule and $\mathcal{H}'_{\rm dip}$ is the interaction between the ith and jth proton pairs with the resultant spin $I = I_1 + I_2$.

First, the intramolecular interaction $\mathcal{H}_{\rm dip}$ will be considered. In the m_I representation the energy is[10]

$$V_{12} = \gamma^2\hbar^2 r_{12}^{-3}(A+B+C+D+E+F), \tag{6}$$

where

$$\begin{aligned} A &= I_{Z1}I_{Z2}(1-3\cos^2\theta_{12}) && (\Delta m=0),\\ B &= -\frac{1}{4}[I_{+1}I_{-2}+I_{-1}I_{+2}](1-3\cos^2\theta_{12}), && (\Delta m=0),\\ C &= -\frac{3}{2}[I_{+2}I_{Z1}+I_{+1}I_{Z2}]\sin\theta_{12}\cos\theta_{12}e^{-i\phi_{12}}e^{i\gamma H_0 t}, && (\Delta m=1), \end{aligned} \tag{7}$$

$$D = -\frac{3}{2}[I_{-2}I_{Z1}+I_{-1}I_{Z2}]\sin\theta_{12}\cos\theta_{12}e^{i\phi_{12}}e^{-i\gamma H_0 t}\ ,\quad(\Delta m=-1)\ ,$$

$$E = -\frac{3}{4}[I_{+1}I_{+2}]\sin^2\theta_{12}e^{-2i\phi_{12}}e^{2i\gamma H_0 t}\ ,\quad(\Delta m=2)\ ,$$

$$F = -\frac{3}{4}[I_{-1}I_{-2}]\sin^2\theta_{12}e^{2i\phi_{12}}e^{-2i\gamma H_0 t}\ ,\quad(\Delta m=-2)\ .$$

A and B terms are secular perturbations and will give the fine structure of the resonance line. In solid hydrogen an asymmetric crystalline potential splits the $J=1$ rotational state of an *ortho* molecule into three sublevels characterized by three wave functions $\psi_\xi\sim\sin\vartheta\cos\varphi$, $\psi_\eta\sim\sin\vartheta\sin\varphi$ and $\psi_\zeta\sim\cos\vartheta$, where ξ, η and ζ are the principal axes of the asymmetric potential. The energy of an *ortho* molecule in the state ψ_ζ is given by[2]

$$\begin{aligned}E_\zeta &= -2\mu_p m_I H_0 - 2\mu_p{}^2 r_{12}{}^{-3}\int(3\cos^2\theta-1)\,\psi_\zeta{}^2 d\tau\cdot(\frac{3}{2}m_I{}^2-1)\\ &= -2\mu_p m_I H_0 - \frac{4}{5}\mu_p{}^2 r_{12}{}^{-3}(3\cos^2\alpha-1)(\frac{3}{2}m_I{}^2-1)\ ,\end{aligned}\qquad(8)$$

where α is the angle between $\mathbf{H}_0$ and the ζ axis. Therefore, the *ortho* molecule in the substate ψ_ζ gives rise to two lines separated by $(1/h)(12/5)\mu_p{}^2 r_{12}{}^{-3}(3\cos^2\alpha-1)$. If the thermally induced transitions between the sublevels are rapid, as would be realized at high temperatures, the dipolar interaction should be averaged over the whole motion and

$$\begin{aligned}E = -2\mu_p m_I H_0 - 2\mu_p{}^2 r_{12}{}^{-3}\int(3\cos^2\theta_{12}-1)(c_\xi\psi_\xi+c_\eta\psi_\eta+c_\zeta\psi_\zeta)^2 d\tau\\ \times(\frac{3}{2}m_I{}^2-1)\ ,\end{aligned}\qquad(9)$$

where $c_\xi{}^2$, $c_\eta{}^2$ and $c_\zeta{}^2$ are proportional to the Boltzmann factors of the respective states and satisfy the condition

$$c_\xi{}^2+c_\eta{}^2+c_\zeta{}^2=1\ .$$

Evidently, the line profile will become complex with narrow overall separation. The former corresponds to the side peaks and the latter to the central peak. The previous researches on the line shape[2],[3] suggested that in powder samples the side peaks had the same separation for each of the rotational sublevels, while the central peak was composed of lines with different separations due possibly to the fact that the local surroundings of different *ortho* molecules are not the same.

The intermolecular interaction $\mathcal{H}'_{\rm dip}$ broadens each level due to the interaction $\mathcal{H}_{\rm dip}$ and gives rise to the line width. The corresponding perturbation V_{ij}' is also decomposed as before,

$$V_{ij}' = \gamma^2\hbar^2 r_{ij}{}^{-3}(A'+B'+C'+D'+E'+F')$$

where

$$A' = I_{Zi}I_{Zj}(1-3\cos^2\theta_{ij})\ ,\qquad(\Delta m=0)\ ,$$

$$B' = -\frac{1}{4}(I_{+i}I_{-j}+I_{-i}I_{+j})(1-3\cos^2\theta_{ij})\ ,\qquad(\Delta m=0)\ ,$$

$$C' = -\frac{3}{2}(I_{+i}I_{Zj}+I_{-j}I_{Zi})\sin\theta_{ij}\cos\theta_{ij}e^{-i\phi_{ij}}e^{i\gamma H_0 t}\ ,\quad(\Delta m=1)\ ,$$

$$D' = -\frac{3}{2}(I_{-i}I_{Zj}+I_{+j}I_{Zi})\sin\theta_{ij}\cos\theta_{ij}e^{i\phi_{ij}}e^{-i\gamma H_0 t}\ ,\quad(\Delta m=-1)\ ,\qquad(10)$$

$$E' = -\frac{3}{4}(I_{+i}I_{+j})\ \sin^2\theta_{ij}\, e^{-2i\phi ij}\, e^{2i\gamma Hot}\ ,\quad (\Delta m=2)\ ,$$

$$F' = -\frac{3}{4}(I_{-i}I_{-j})\ \sin^2\theta_{ij}\, e^{+2i\phi ij}\, e^{-2i\gamma Hot}\ ,\quad (\Delta m=-2)\ .$$

If the m_I levels of all the *ortho* molecules are equidistant, the terms A' and B' will become secular perturbations, both contributing to the line width. The corresponding second moment is given by the Van Vleck's formula,[16] that is,

$$<\Delta\nu^2>_{AV} = \frac{3}{4} I(I+1)\,\gamma^4\hbar^2 \sum_j (1-3\cos,^2\theta_{ij})^2 r_{ij}^{-6}\ . \qquad (11)$$

Owing to the perturbation $\mathfrak{H}_{\rm dip}$, however, the levels are not equidistant and the B' term, which provides the simultaneous flip-flop of the two spins i and j, is not, in general, the secular perturbation. Two typical examples of the level diagram of the *ortho* molecules in solid hydrogen shown in Fig. 13 will be considered:

Case (a). When the molecules i, j have the same level diagram as shown in Fig. 13a, a part of the B' term becomes semi-diagonal. The flip-flop, $m_i = +1 \to 0$ and $m_j = 0 \to +1$, is possible without net change of the energy, while the flip-flop, $m_i = +1 \to 0$ and $m_j = -1 \to 0$, does not conserve the energy. The corresponding second moment can be calculated by the method of Ishiguro et al[15] and is smaller by a factor 5/6 than that of the equidistant case given by (11). The side peak will belong to this case.

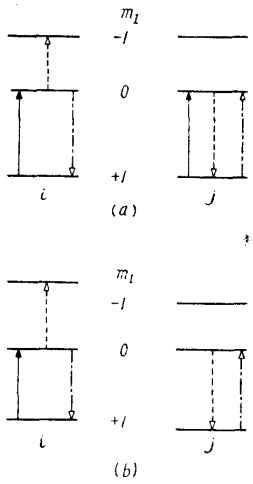

Fig. 13. Magnetic energy level diagrams for of the ortho molecules (I = 1) in solid hydrogen, Solid lines represent the *rf* induced transitions, dotted and chained lines represent the simultaneous flip-flops between two proton pairs.

Case (b). If the ith and jth molecules have quite different energy level diagrams as sketched in Fig. 13b, the B' term can no longer be semi-diagonal. The second moment is reduced by a factor 4/9, compared with the equidistant case[16]. The central peak will fall under this case.

When the internal equilibrium between equidistant spin levels is disturbed by resonance absorption of energy from the *rf* field, the recovery will be attained by the spin-spin interaction B'. However, the problem is not simple in a system having non-equidistant spin levels. In the case shown in Fig. 13b the equilibrium cannot be established, provided that the spins do not couple with the lattice, because the mutual flip-flops indicated by dotted and chained lines are non adiabatic. The mechanism of spin-lattice interaction in solid hydrogen, therefore, must be studied in detail.

(15) E. Ishiguro, K. Kamde and T. Usi, Physica, **17** (1951), 310.
(16) J. H. Van Vleck, Phys. Rev., **74** (1948), 1168.

VI. Spin-lattice interaction

The following will be considered as the mechanism of coupling between the spin system and the lattice in solid hydrogen:

(1) modulation of the proton-proton interaction between *ortho* molecules by lattice vibrations,

(2) modulation of the dipolar interaction in an *ortho* molecule by molecular rotation,

(3) modulation of the interaction of the nuclear spin with the electron spin by a change in electron spin orientation or modulation of the interaction of the nuclear spin with the rotational magnetic moment by a change of the rotational axis of an *ortho* molecule. Of these, the cases (2) and (3) will be important, because the case (1) gives rise to a very long relaxation time[17].

The mechanism (2), which is the most important one, will be considered by using the expression (7). When the thermal motion of the crystal lattice induces transitions between the sublevels of the rotational state $J=1$, the terms C, D, E and F become responsible for spin-lattice relaxation. According to the simple theory developed by BPP, the relaxation time T_1 is given in terms of the Fourier spectrum of the position functions involved in these terms, that is,

$$\frac{1}{T_1}=\frac{3}{2}\gamma^4\hbar^2 I(I+1)\left[J_1(\nu)+\frac{1}{2}J_2(2\nu)\right]. \tag{12}$$

It will be assumed that the direction of the molecular axis will vary in a random fashion with a correlation time τ_c. Then, $J(\nu)$'s are written as follows:

$$\begin{aligned} J_1(\nu) &= <F_1(t)^*F_1(t)>_{AV}\ 2\tau_c(1+4\pi^2\nu^2\tau_c^2)^{-1}, \\ J_2(2\nu) &= <F_2(t)^*F_2(t)>_{AV}\ 4\tau_c(1+16\pi^2\nu^2\tau_c^2)^{-1}, \end{aligned} \tag{13}$$

where

$$\begin{aligned} F_1 &= \sin\theta_{12}\cos\theta_{12}e^{i\phi_{12}}r_{12}^{-3}, \\ F_2 &= \sin\theta_{12}e^{2i\phi_{12}}r_{12}^{-3}. \end{aligned} \tag{14}$$

In the central peak $F^*(t)F(t)$ should be averaged over the motion specified by the wave function $\Psi=c_\xi\psi_\xi+c_\eta\psi_\eta+c_\zeta\psi_\zeta$. As the mixing ratio of the three sublevel functions depends upon the asymmetry of the crystalline potential, the average will not be the same for each of the *ortho* molecules. Therefore, each molecule has its own $<F^*F>_{AV}$, which, however, will not differ widely from each other. $<F^*(t)F(t)>_{AV}$ of the side peak, on the contrary, may be the same for all the molecules, because the transitions between sublevels will be rare in the ordered state.

The correlation time τ_c implys the life time of a sublevel of the state $J=1$ and its reciprocal is related to the probability of transition between sublevels, which will be induced by the thermal vibrations of the lattice or by the flip-flops of the rotation axes of *ortho* molecules analogus to the flip-flops of spins due to the

(17) I. Waller, Zeits. f. Phys., **79** (1932), 380.

interaction B'. Theoretical study of such transition would be necessary for the complete understanding of the mechanism of spin-lattice relaxation, though it is beyond the scope of the present research. Since in the present case only a qualitative discussion on τ_c is concerned about, we shall be contented with the results of an crude estimation by Reif[2]. According to him, the probability of the transition induced by thermal vibrations is

$$W_{\zeta\eta} = 10^6 T^3 [\exp(\Delta E_{\zeta\eta}/kT - 1)]^{-1}, \tag{15}$$

where $\Delta E_{\zeta\eta}$ is the energy gap between respective sublevels and $W_{\zeta\eta}$ is the probability of transition between them. The mean correlation time of an *ortho* molecucle will be,

$$\bar{\tau}_c = 10^{-6} T^{-3} <\exp(\Delta E/kT - 1)>_{AV}, \tag{16}$$

where the average must be taken over all the transitions of the molecule. This relation shows that τ_c becomes longer as the gap ΔE becomes larger. Inserting this into Eq. (12) we obtain, for instance when $\bar{\tau}_c \nu \geq 1$,

$$1/T_1 = \frac{3}{2}\gamma^4\hbar^2 I(I+1) <F^*(t)F(t)> \{2(2\pi\nu)^{-2}10^6 T^3 <\exp(\Delta E/kT - 1)>_{AV}^{-1}$$
$$+2(4\pi\nu)^{-2}10^6 T^3 <\exp(\Delta E/kT - 1)>_{AV}^{-1}\}. \tag{17}$$

It is evident from this relation that T_1 should be different for different *ortho* molecules, as ΔE's are not the same for each of these molecules owing to the inhomogeneous nature of the crystal, and that T_1 of a component near the line center should be shorter than that of the distant one, because the narrow component comes from molecules with small ΔE[3]. Molecules with like local surroundings should have the same T_1 and, consequently, show the same saturation behavior.

In the above, spin-lattice relaxation of the central peak has been considered. The argument, however, will not be applicable to the side peak where ortho molecules are in a state of rotational order. At present there is no reasonable mechanism of spin-lattice relaxation in this case, but it may be safe to suppose that T_1 will have the same value over the whole crystal.

Finally, the effect of spin-diffusion upon the relaxation time will be discussed This has been recognized as an important mechanism of spin-lattice relaxation in many crystals[18]. Simultaneous flip-flops of spins due to the interaction B'_{ij} of Eq. (10) enable the absorbed energy to be transfered to nuclei which are maintained at the temperature of the lattice by the strong interaction with paramagnetic impurities. As a consequence of this fact, T_1 of the crystal is determined by the nuclear spin-diffusion rate or the relaxation time of the impurities. In the present case, a trace of oxygen or the ortho molecules with very short T_1 will play the role of impurity. However, as the spin-diffusion is, in general, forbidden in solid hydrogen from the reasons described in section V, T_1 will not be affected by those impurities. Therefore, it can be expected that a distribution of T_1 will be found from the saturation curve of the central peak even if the crystal contains paramagnetic impurities.

(18) N. Bloembergen, Physica, **15** (1949), 380.

VII. Theory of anomalous saturation and the spin-lattice relaxation time

The foregoing arguments suggest that in the central peak the spin system as a whole cannot relax with a single relaxation time. The saturation behavior, then, would not be explained by the results of the simple theory. A theoretical treatment of the saturation is necessary for the purpose of obtaining the relaxation time from the present experimental data.

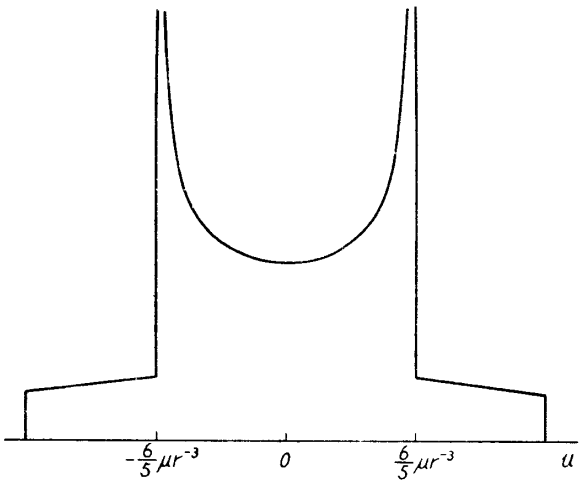

Fig. 14. Line shape function $p(u)$ of the side peak in solid hydrogen. The abscissa u is the deviation of the resonance frequency ν from the center ν_0, $u=\nu-\nu_0$.

First, the saturation behavior of the side peak will be considered, as this case seems to be simpler than that of the central peak. It may be assumed that in a single crystal all the *ortho* molecules are in the lowest rotational sublevel ψ_ζ. The direction of the ζ axis will be the same over the crystal or the same at least over a single domain in it. According to Eq. (8), the resonance line has two peaks separated by

$$(1/h)\ (12/5)(\mu_p^2 r_{12}^{-3})(3\cos^2\alpha-1)\,,$$

each having an intensity distribution function $g(\nu)$ due to intermolecular dipole-dipole interaction $\mathfrak{H}'_{\rm dip}$. Eq. (1) can be applied to the saturation of each peak and

$$\chi''(\nu,H_1)=\frac{\pi}{2}\chi_0\nu\frac{g(\nu)}{1+\frac{1}{2}\gamma^2H_1^2T_1g(\nu)}\,.$$

In our polycrystalline sample, however, the whole line shape is determined by a shape function $p(\nu-\nu_0)$, which is normalized so that

$$\int_0^\infty p(\nu-\nu_0)=1\,,$$

where ν_0 is the resonance frequency at the line center. $p(\nu-\nu_0)$ has been calculated by Reif[2] and is reproduced in Fig. 14. Remembering the results of Sections V and VI, the imaginary susceptibility can be expressed in the form,

$$x''(\nu,H_1)=\frac{\pi}{2}\chi_0\int_0^\infty p(\nu'-\nu_0)\frac{\nu'g(\nu-\nu')}{1+\frac{1}{2}\gamma^2H_1^2T_1g(\nu-\nu')}d\nu'\,. \tag{18}$$

Here T_1 is considered as being the same for all the nuclei in the crystal. In the experiment saturation was measured on the meter deflection of the "lock in" out-put, which is given by

$$D \propto \frac{dx''(\nu, H_1)}{d\nu} = \frac{\pi}{2}\chi_0 \frac{\partial}{\partial \nu}\left[\int_0^{\infty} p(\nu'-\nu_0)\frac{\nu' g(\nu-\nu_1)}{1+\frac{1}{2}\gamma^2 H_1^2 T_1 g(\nu-\nu,)}d\nu'\right]$$

$$= \frac{\pi}{2}\chi_0 \frac{\partial}{\partial x}\left[\int_{-\infty}^{+\infty} p(u-x)\frac{g(x)}{1+\frac{1}{2}\gamma^2 H_1^2 T_1 g(x)}dx\right], \qquad (19)$$

where $x = \nu - \nu'$ and $u = \nu - \nu_0$. Two cases must be distinguished according as T_1 is larger or smaller than the modulation frequency ν_m:

Case 1 $2\pi\nu_m T_1 > 1$,

$$D \propto \int p(u-x)\frac{1}{1+\frac{1}{2}\gamma^2 H_1^2 T_1 g(x)}\frac{dg(x)}{dx}dx\,, \qquad (20,\text{a})$$

Case 2 $2\pi\nu_m T_1 < 1$,

$$D \propto \int p(u-x)\frac{d}{dx}\left(\frac{g(x)}{1+\frac{1}{2}\gamma^2 H_1^2 T_1 g(x)}\right)dx\,. \qquad (20,\text{b})$$

For $g(x)$ a Gaussian may be assumed as usual:

$$g(x) = g_0 \exp(-x^2/2\beta^2)\,,$$

where

$$g_0 = \frac{1}{\sqrt{2\pi}\,\beta} = \frac{1}{\sqrt{2\pi}}\frac{1}{\sqrt{<\Delta\nu^2>_{AV}}}\,.$$

$<\Delta\nu^2>_{AV}$ is the second moment of the component line and is given by

$$<\Delta\nu^2>_{AV} = c\cdot(2\mu_p)^4 h^{-2}\sum_j r_{ij}^{-6}\,, \qquad (21)$$

where c is the *ortho* concentration and r_{ij} is the intermolecular distance, 3.75 Å. The theoretical saturation curve calculated from (20, a) is in good agreement with the experimental curve shown in Fig. 5. This fact suggests that the relaxation times are the same for different *ortho* molecules in the side peak. The following relation is obtained from the theoretical curve,

$$D_{\max}(H_1)/D_{\max}(0) = 0.68 \qquad (22)$$

when $\frac{1}{2}\gamma^2 H_1^2 T_1 g_0 = 1$.

The relaxation time can be calculated from the experimental saturation curve by using the above relation. The result is given in Table 1. As the saturation curves at temperatures between 1.4° and 1.2°K coincide with the one shown in Fig. 5 within the experimental error, the values of T_1 at these temperatures may be considered to be the same.

Saturation curves of the central peak show very complicated behaviors depending upon the *ortho* concentration and temperature and cannot be explained by the above considerations. This must be attributed mainly to the distribution of T_1. In this case the imaginary susceptibility is given by

$$\chi''(\nu, H_1) = \frac{\pi}{2}\chi_0 \int\int p(\nu'-\nu_0) f(\lambda)\frac{\nu' g(\nu-\nu')}{1+\frac{1}{2}\gamma^2 H_1^2 T_1(\lambda) g(\nu-\nu')}d\nu' d\lambda\,, \qquad (23)$$

Table 1. Spin-lattice relaxation time in solid hydrogen.

Side peak		
Ortho concentration %	Temperature °K	Spin-lattice relaxation time, T_1 sec
69±2	1.25	0.23

Central peak			
Ortho concentration %	Temperature °K	Spin-lattice relaxation time	
		T_1 (maximum) sec	T_1 (minimum) sec
71±2	4.2	0.29	$2.1\cdot10^{-3}$
66±2	4.2	0.34	$1.8\cdot10^{-3}$
52±2	4.2	0.38	$1.8\cdot10^{-3}$
61±2	2.35	0.88	$1.3\cdot10^{-3}$
65±2	1.95	0.92	$1.4\cdot10^{-3}$
69±2*	1.25	1.2	$1.7\cdot10^{-3}$
63±2	1.25	1.3	$1.3\cdot10^{-3}$
49±2	1.25	1.4	$1.3\cdot10^{-3}$

* Central peak coexisting with the side peaks.

where T_1 is considered to be a function of a parameter λ, whose distribution function is $f(\lambda)$, and $p(\nu'-\nu_0)$ is the line shape function of the central peak. According to the simple consideration made in section VI, T_1 is related to the distance of the component line from the center and, therefore, may be written as

$$T_1(\lambda) \propto (\nu-\nu_0)^n = u^n \qquad n\text{: integer.} \tag{24}$$

The line shape function $p(\nu-\nu_0)$ can be regarded as a superposition of that of the side peaks with different separations and may be approximated by a curve shown in Fig. 15a. When $\lambda = u$, a function like $p(u)$ shown in Fig. 15a can be used as $f(u)$. With these assumptions the theoretical derivative curves are calculated from the formula:

Case 1 $2\pi\nu_m T_1 > 1$,

$$D \propto \int_{-\infty}^{+\infty} p(u-x) \frac{1}{1+\frac{1}{2}\gamma^2 H_1^2 T_1(u) g(x)} \frac{dg(x)}{dx} dx, \tag{25, a}$$

Case 2 $2\pi\nu_m T_1 < 1$,

$$D \propto \int_{-\infty}^{+\infty} p(u-x) \frac{d}{dx}\left(\frac{g(x)}{1+\frac{1}{2}\gamma^2 H_1^2 T_1(u) g(x)} \right) dx, \tag{25, b}$$

where $T_1(u) = \text{const} \cdot u^n$ and $g(x) = g_0 \exp(-x^2/2\beta^2)$. The results of calculations* by Eq. (25,a) are illustrated in Figs. 15b and 16. Fig. 15b shows the variation of the line shape with increasing saturation, which is in accord with the observation shown in Fig. 2. Calculated derivatives at several points from the line center is plotted against H_1 (in arbitrary unit) in Fig. 16. The theoretical saturation curves

* In the calculation, the value of T_1 at $-0.5\beta < u < 0.5\beta$ was taken as one tenth of the maximum T_1 at $u = \pm 3\beta$ and β was assumed as 1 gauss.

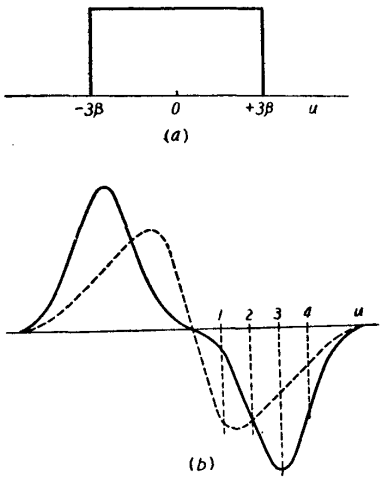

Fig. 15. a) Assumed line shape function $p(u)$ for the central peak and b) calculated derivatives with a component line broadening function, $g(x)=g_0\exp(-x^2/2\beta^2)$, for two values of the saturation factor $S=\frac{1}{2}\gamma^2H_1^2T_{1,\max}g_0$.

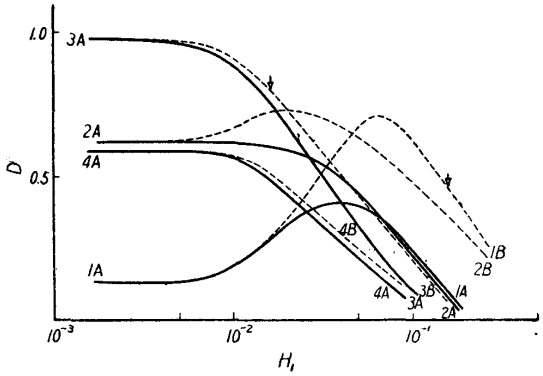

Fig. 16. Theoretical saturation curves of the derivatives shown in Fig. 15. Solid and dotted lines correspond to the cases: $T_1\propto u$ and $T_1\propto u^2$.

for $n=2$ resemble, in shape, to those in 71 per cent hydrogen shown in Fig. 6. It must be noted that an agreement with the experiment is obtained only when T_1 is assumed to be a function of the separation u. It can be concluded, therefore, that a distribution of T_1 exists in the central peak, and that T_1 is approximately expressed by a relation $T_1\propto u^n$ with $n\sim 2$. The following relations are obtained from the calculated saturation curves for $n=2$:

from Curve 3B

$$D(\nu,H_1)/D(\nu,o)=0.80 \qquad \text{for} \qquad \frac{1}{2}\gamma^2H_1^2T_{1,\max}g_0=1, \tag{26,a}$$

from Curve 1B

$$D(\nu,H_1)/D(\nu,o)=0.67^* \qquad \text{for} \qquad \frac{1}{2}\gamma^2H_1^2T_{1,\min}g_0=1. \tag{26,b}$$

These relations are not necessarily hold good for another form of the distribution function of T_1 and consequently cannot be applied to all the cases. The above criterion was tentatively applied to all the experimental saturation curves of the central peak, as the real distribution functions of T_1 in every case are unknown. The maximum value of T_1 was calculated from curves 3 or 4 by using the relation (26, a), while, the minimum value was obtained from curves 1 or 2 by using the formula (26, b). For g_0, the following expression was used as before:

$$g_0=\frac{1}{\sqrt{2\pi}}\,\frac{1}{\sqrt{<\Delta\nu^2>_{AV}}},$$

where the second moment $<\Delta\nu^2>_{AV}$ is given by (see the case b, p. 103)

$$<\Delta\nu^2>=c\cdot\frac{8}{15}(2\mu_p)^4h^{-2}\textstyle\sum_j r_{ij}^{-6}.$$

* This value is not valid for the case of short T_1 as in this case Eq. (25, b) should be used instead of Eq. (25, a). However, the error seems not to be so large.

where c is the ortho concentration and $r_{ij} = 3.75$Å. The upper and lower limits of T_1 thus obtained are shown in Table 1. They are valid only in the order of magnitude. It must be noticed that the ratio of the maximum T_1 to the minimum is approximately 100 : 1 at 4.2°K and that the maximum is nearly inversely proportional to temperature and ortho concentration. The distribution functions of T_1 seem to be different from each other depending upon the ortho concentration and the temperature. As seen from Figs. 11 and 6, the absorption line in 49 per cent hydrogen can be regarded as a superposition of a peak whose components have nearly the same T_1 ($\sim T_{1,\max}$) and a peak whose components have different T_1 depending on their separations from the line center, while the line consists only of the latter in 71 per cent hydrogen at 4.2°K.

VIII. Discussions and remarks

It has been confirmed experimentally that the saturation of the absorption peaks in solid hydrogen is not homogeneous, and that the spin-lattice relaxation time has widely distributed values in the disordered state of molecular rotation. The spin-lattice relaxation times of Table 1 is in disagreement with those reported by Hatton and Rollin[1] given in Table 2. Since they assumed the saturation of the central and the side peak being homogeneous, discrepancies between their results and the present ones seems to be quite natural. If the saturation of the central peak were normal and homogeneous, the relaxation time would have a single value over the whole crystal, because the absorbed energy would be transfered by spin diffusion to the nuclei where the spin-lattice interaction is strong enough[18].

Table 2. Spin-lattice relaxation time in normal solid hydrogen according to Hatton and Rollin[1]

Temperature °K	4.2	1.85	1.3	1.1
T_1 sec	0.3	0.5	2	2

The difference between the homogeneous and the inhomogeneous saturations will be made clear when the present data on the side peak is compared with those of Hatton. T_1 of the side peak in normal hydrogen was 2 seconds at 1.3° and 1.1°K in Hatton's experiment, while it was 0.2 second at 1.25°K in the present case. If the concept of homogeneous saturation is applied to the present data, a relaxation time of about 3 seconds which is in agreement with Hatton's value, is obtained instead of 0.2 second.

Though the conclusions about the mechanism of spin-lattice relaxation are based on some assumptions and seem to be of only qualitative significance, it may be certain that T_1 of the central peak is related to the magnitude and the anisotropy of the crystalline potential. A more complete theory of the spin-lattice relaxation based on an exact description of the crystalline potential corresponding to the local *ortho-para* arrangements would be able to derive the distribution function

of T_1 from the experiment. Such a theory is highly desirable for the more detailed account of the anomalous saturation. At any rate, the above-mentioned anomalous saturation is not only an interesting problem in the nuclear magnetic resonance, but also is an important key to the problem concerning the nature of solid *ortho-para* hydrogen.

Acknowledgements

The present author would like to express his gratitude to Professor E. Kanda for his support and stimulating discussions throughout this work, and also to Dr. R. W. Hill of the Clarendon Laboratory, University of Oxford, for his kind communication about his experimental results. Analysis of the sample was kindly made by Miss H. Kobayashi and many of the measuring equipments were constructed by Mr. H. Sato. The author wishes to express his thanks for their assistance.